

Published in final edited form as:

*Science*. 2018 June 29; 360(6396): 1469–1473. doi:10.1126/science.aas9408.

## Sex reversal following deletion of a single far upstream enhancer of *Sox9*

Nitzan Gonen<sup>1</sup>, Chris R Futtner<sup>2</sup>, Sophie Wood<sup>1</sup>, S. Alexandra Garcia-Moreno<sup>2</sup>, Isabella M Salamone<sup>2,3</sup>, Shiela C Samson<sup>1,4</sup>, Ryohei Sekido<sup>5,6</sup>, Francis Poulat<sup>7</sup>, Danielle M Maatouk<sup>2</sup>, and Robin Lovell-Badge<sup>1,\*</sup>

<sup>1</sup>The Francis Crick Institute, 1 Midland Road, London NW1 1AT, UK

<sup>2</sup>Department of Obstetrics and Gynecology, Northwestern University, Chicago, IL 60611, USA

<sup>5</sup>Institute of Medical Sciences, University of Aberdeen, Foresterhill, Aberdeen AB25 2ZD, UK

<sup>7</sup>Department of Genetics and Development, Institute of Human Genetics, CNRS-University of Montpellier UMR9002, Montpellier, France

### Abstract

Cell fate decisions require appropriate regulation of key genes. *Sox9*, a direct target of SRY, is pivotal in mammalian sex determination. *In vivo* high-throughput chromatin accessibility techniques, transgenic assays, and genome editing revealed several novel gonadal regulatory elements in the 2 Mb gene desert upstream of *Sox9*. Although others are redundant, Enh13, a 557 bp element located 565 kb 5', is essential to initiate mouse testis development; its deletion giving XY females with *Sox9* transcript levels equivalent to XX gonads. Our data is consistent with the time-sensitive activity of SRY and indicates a strict order of enhancer usage. Enh13 is conserved and embedded within a 32.5 kb region whose deletion in patients is associated with XY sex reversal, suggesting it is also critical in humans.

---

The regulation of genes with important roles in embryonic development can be complex, involving multiple, often redundant enhancers, repressors, and insulators (1, 2). The genes may have a poised epigenetic state prior to their expression, and their activation or repression may involve positive or negative feed forward loops. This complexity is likely to be amplified when the gene has functions in more than one tissue, given that the regulatory

---

\*Corresponding author: robin.lovell-badge@crick.ac.uk.

<sup>3</sup>Current addresses: Center for Genetic Medicine, Northwestern University, Chicago, IL, 60611, USA.

<sup>4</sup>Current addresses: Department of Oncological Sciences, Huntsman Cancer Institute, University of Utah, Salt Lake City, UT 84112 USA.

<sup>6</sup>Current addresses: Institute of Ophthalmology, University College London, 11-34 Bath Street, London EC1V 9EL.

**Author contribution:** N.G and R.L.B designed the study. C.R.F, S.A.G.M, I.M.S and D.M.M performed ATAC-seq, H3K27ac ChIP-seq and cloned the Enhancer-LacZ plasmids. S.C.S helped with analysing the reporter mice. S.W performed cytoplasmic and pronuclear zygote injections. R.S provided the TESMS-CFP mice. F.P performed the mouse and bovine SOX9 and SRY ChIP. N.G performed the rest of the experiments. N.G and R.L.B analysed and interpreted the results and wrote the manuscript. All authors reviewed and added input to the manuscript.

**Competing interests:** Authors have no competing interests.

**Data and materials availability:** All data are available in the manuscript or the supplementary materials. ATAC-seq and H3K27Ac ChIP-seq data have been deposited in the Gene Expression Omnibus under accession number GSE99320

elements required for each are often interspersed and necessitate dynamic alterations in chromatin conformation (1, 2). The developing gonads comprise an interesting system in which to explore questions of gene regulation during development (3). Most of the cell lineages are bipotential with the ability to give rise to cell types typical of either ovaries or testes and many genes that become associated with male or female fate begin by being expressed at equivalent, although usually low levels, in supporting cell precursors of both XX and XY gonads (4–6).

In mammals, the *Sry* gene encodes a protein that is transiently expressed and initiates testis and subsequent male development by triggering cells of the supporting cell lineage to differentiate into Sertoli rather than granulosa cells typical of ovaries (7). *Sox9*, the main target of SRY, is critical for the differentiation of Sertoli cells and then functions along with other transcription factors, notably *Sox8* and then *Dmrt1* for their maintenance (4–6). Both gain and loss of function studies in mouse and human demonstrate that *Sox9* plays a key role in testis determination (8–13). Notably, humans, heterozygous for null mutations develop campomelic dysplasia (CD, OMIM 114290) (11), a severe syndrome where 70% of XY patients show female development (12, 13).

*Sox9* functions in many embryonic and adult cell types (14), and genetic and molecular evidence suggests that its regulatory region is spread over at least a 2 Mb gene desert 5' to the coding sequence (15). The only enhancer known to be relevant for expression in Sertoli cells was TES, a 3.2 kb element mapping 13 kb 5', and its 1.4 kb core, TESCO (16). Targeted deletion of TES or TESCO reduced *Sox9* expression levels in the early and postnatal mouse testis to about 45% of normal but did not result in XY female development (17). We therefore used several unbiased approaches to systematically screen for additional gonad enhancers upstream of mouse *Sox9*. We first made use of DNaseI-seq data obtained with E13.5 and E15.5 sorted Sertoli cells (18). From 33 putative enhancers we chose only those positive at both stages for *in vivo* validation by transgenic assays (14 enhancers, Fig. 1A and fig. S1). In parallel we carried out ATAC-seq on XY and XX gonads, which permitted the use of fewer sorted cells at E10.5, an early bipotential stage, and E13.5, when gonadal sex is already determined (fig. S1, S2 and methods). Most putative enhancers discovered by DNaseI-seq were evident in the E13.5 XY ATAC-seq data, however we used this to include two more in the *in vivo* screen; Enhancer (Enh) 1 and 14 (Fig. 1A and fig. S1). Chromatin immunoprecipitation-seq (ChIP-seq) was also performed for H3K27ac, a histone modification that marks active enhancers (fig. S1).

All 16 putative enhancers were cloned upstream of an *hsp68* minimal promoter and the reporter gene *LacZ*, and used to generate transgenic mice (2, 19) (Table 1). For initial screens we performed transient analyses at E13.5. Twelve failed to give any gonadal  $\beta$ -Galactosidase ( $\beta$ -Gal) activity, although many showed staining in other tissues in which *Sox9* is normally expressed, such as chondrocytes, brain, and spinal cord (fig. S3). The remaining four showed gonad expression and these constructs were re-injected to generate stable lines in order to better study their activity in both males and females during development. Enh8 (672 bp-long, 838 kb 5') conferred robust  $\beta$ -Gal activity in the ovary, whereas it was barely present in the testis at E13.5 (Fig. 1A and fig. S4B). This may be due

to Enh8 being taken out of its original genomic context; notably ATAC-seq reveals a much stronger peak in granulosa cells compared to Sertoli cells (fig. S4A).

In contrast, Enh14 (1287 bp-long, 437 kb 5') showed robust testis specific  $\beta$ -Gal activity (Fig. 1A and fig. S5B). DNaseI-seq, ATAC-seq, and H3K27ac ChIP-seq all suggest that this enhancer is active and open only in Sertoli cells (fig. S1 and S5A). To test this candidate, we used genome editing to delete Enh14. However, Enh14 deletion did not alter expression of *Sox9*, its target gene *Amh*, or *Foxl2*, a marker of granulosa cells, in E13.5 XY gonads (fig. S5D), indicating that Enh14 has a redundant role, at least in the embryo. Enh32 (970 bp-long, 10 kb 5') is also testis-specific, but very weak and restricted to a domain close to the mesonephros (Fig. 1A and fig. S6B-C). ATAC-seq, DNaseI-seq, and H3K27ac ChIP-seq data suggest that this is a Sertoli-cell enhancer, although weak peaks were seen in the granulosa cell samples (fig. S1 and S6A).

The remaining enhancer, Enh13 (557 bp-long, 565 kb 5'), is highly conserved among mammals and located towards the distal 5' end of a 25.7 kb region in mice showing conserved synteny with a 32.5 kb region upstream of human *SOX9* termed XY SR, whose deletion is associated with sex reversal (20) (Fig. 1A-B and fig. S1). Enh13 shows the strongest Sertoli cell-specific peak within this region, in both the DNaseI-seq and ATAC-seq data. H3K27ac ChIP-seq data marks Enh13 as active in both Sertoli and granulosa cells, which may support the observation that some transgenic lines also exhibit  $\beta$ -Gal activity in the ovary (Fig. 1C and fig. S1, S7A).  $\beta$ -Gal expression is clearly within Sertoli and granulosa cells (fig. S7C). ATAC-seq data from E10.5 genital ridges shows that Enh13 is not open at this stage, irrespective of chromosomal sex (Fig. 1B and fig. S1), suggesting that it opens co-incident with specification of the supporting cell lineage from SF1-positive cells of the coelomic epithelium (5).

Genome editing was used to derive mice homozygous for deletions of Enh13. Irrespective of whether this was carried out on a TES mutant background or by itself it always led to XY female development (Fig. 2, fig S8-10). The latter result was surprising, because if TES accounts for 55% of *Sox9* expression in early Sertoli cells, any additional enhancer(s) should not account for more than 45%, and, when deleted, levels of *Sox9* would remain higher than the threshold of about 25% below which sex reversal might be expected (17). Nevertheless, at embryonic stages, whereas XY Enh13<sup>+/-</sup> embryos still undergo normal testis development, XY Enh13<sup>-/-</sup> embryos produce ovaries indistinguishable from those of XX wild type embryos, with no signs of testis cords or a coelomic vessel (Fig. 2B-C and fig. S10). Immunofluorescence analysis for SOX9 and FOXL2 of E13.5 and 6-week-old XY Enh13<sup>+/-</sup> and Enh13<sup>-/-</sup> gonads showed that the former are still testes whereas the latter are fully sex reversed ovaries (Fig. 2C and fig. S10D). Similar analysis of XX Enh13-deleted gonads did not show any obvious phenotype (fig. S11).

The Enh13 deletion was generated on a C57BL/6J genetic background, which is sensitized towards XY female sex reversal (21). To test the strength of the deleted allele, we therefore backcrossed it onto a mixed C57BL/6J x CBA background. As before, XY heterozygotes presented as normal fertile males whereas homozygotes showed full male-to-female sex reversal (fig. S12).

We could detect no difference in gonadal phenotypes between *Enh13*<sup>-/-</sup>:*TES*<sup>+/+</sup> and *Enh13*<sup>-/-</sup>:*TES*<sup>-/-</sup> embryos or mice, suggesting that homozygosity for the *Enh13* deletion alone reduced *Sox9* levels well below the critical threshold required for testis development, which had been determined at E13.5 (17) (fig. S8, S10). However, examining levels of gene expression at this stage when there is sex reversal will be uninformative because factors such as *WNT4* and *FOXL2* repress *Sox9* once ovary development begins (5). We therefore analysed *Sox9*, *Sry*, *Sf1* and *Foxl2* mRNA at E11.5, during the brief period when gonadal sex is being determined. qRT-PCR revealed that XY *Enh13*<sup>+/-</sup> and *Enh13*<sup>-/-</sup> genital ridges expressed 58% and 21% of the wild type levels of *Sox9* mRNA, whereas XY *TES*<sup>+/-</sup> and *TES*<sup>-/-</sup> genital ridges showed 55% and 50% respectively (Fig. 3A). In control genital ridges, XX contained 18% of the *Sox9* mRNA levels found in XY (Fig. 3A). Therefore, E11.5 XY *Enh13*<sup>-/-</sup> gonads express *Sox9* at levels close to those of XX gonads at the same stage, explaining the observed complete sex reversal. Deleting one or two copies of *TES* had relatively little effect at E11.5, especially compared to at E13.5, and is in contrast to the results with *Enh13* deletions at E11.5 (Fig. 3A) (17). This again supports the conclusion that *Enh13* plays a more significant role than *TES* during early gonadal development.

*Sry* expression is normally downregulated as *SOX9* levels increase, but it can persist if testis differentiation fails (22, 23). This is consistent with a direct or indirect repressive effect of *SOX9* on *Sry*. At E11.5, *Sry* mRNA levels were higher compared to wild type in both *Enh13*<sup>+/-</sup> and *Enh13*<sup>-/-</sup> XY gonads (168% and 152% respectively, Fig. 3B). In contrast, the *TES* deletion did not significantly alter *Sry* expression (Fig. 3B), which is expected because Sertoli cell differentiation is proceeding in these mutants. *SF1* is known to interact first with *SRY* and later with *SOX9* to regulate *Sox9* expression levels and also many of their downstream target genes (16). We found no significant changes in levels of *Sf1* mRNA in any of the enhancer deletions at E11.5 (Fig. 3C). Using *Foxl2* as an early marker of granulosa cell differentiation (24), mRNA levels were 3.6-fold higher in XX than XY wild type gonads at E11.5 (Fig. 3D). Compared to the latter, *Enh13*<sup>+/-</sup> and *Enh13*<sup>-/-</sup> XY gonads showed a 2-fold and 3-fold increase, respectively, with the homozygotes having very close to XX control levels. Therefore, *Enh13*<sup>-/-</sup> XY gonads reveal an early commitment to the ovarian pathway.

There was a 30-50% decrease in *Sox9* mRNA levels in E11.5 XX *Enh13*<sup>-/-</sup> gonads compared to wild type, reflected by reduced immunofluorescence for *SOX9* protein (fig. S11). These data indicate that *Enh13* also plays a role in the very early expression of *Sox9* in the XX gonad, consistent with both the small peak seen with ATAC-seq and with occasional reporter activity in the transgenic mouse assays (Fig. 1B-C and fig. S7).

The sequence of *Enh13* is highly conserved among mammals (Fig. 1B), and contains consensus binding sites for transcription factors known to regulate early gonad development and sex determination (fig. S13) (6). Mouse *Enh13* contains a single consensus *SRY* binding site as well as a *SOX9* site to which *SRY* can also bind (Fig. 4A, fig. S13). ChIP-qPCR on E11.5 gonads dissected from *Sry-Myc* transgenic embryos was performed using a specific antibody against the *MYC* tag (22). There was an 11-fold enrichment in *SRY-MYC* positive versus negative gonads with primers spanning the *SOX9* consensus site and a 6-fold enrichment with primers spanning the *SRY* site, whereas primers against the strongest *SRY*

binding site in TESCO (22) showed 5-fold enrichment (Fig. 4A-B). This reveals the strong binding of SRY to Enh13 at E11.5, with a preference for the SOX9 consensus site, possibly due to the adjacent SF1 binding site. Preferential binding of SRY to Enh13 over TESCO at E11.5 supports the hypothesis that the former is more critical because it initiates upregulation of *Sox9* while the latter is secondary.

ChIP assays revealed SOX9 to be bound at similar levels to both Enh13 and TESCO in cells from E13.5 testes (Fig. 4C). In addition, SOX9 ChIP-seq data using bovine embryonic testis (25) revealed a strong peak localizing to the conserved syntenic region of Enh13 (537 bp-long, 570 kb 5', Fig. 4D). This suggests that, like TES, Enh13 is used by SOX9 to autoregulate its expression, and that this interaction is conserved in mammals. Unlike several other gonadal enhancers, Enh13 appears well conserved, has a clear role in mice to initiate upregulation of *Sox9* expression, in response to SRY activity, and it may contribute to its maintenance. This makes it very likely to play a similar role in humans given its location within the XYSR region (20, 26). If so, heterozygosity for Enh13 deletions in humans should mimic heterozygosity for null mutations in SOX9 with XY female sex reversal occurring in about 70% of cases, but perhaps without other CD phenotypes.

It is clear from our data and that of others that the upstream regulatory region of *Sox9* is very complex. Our screens using gonadal cells revealed 33 potential enhancers distributed over 1.5 Mb. Transgenic assays used to test the most promising 16, revealed four that gave expression in the gonads, whereas the majority did not. This “hit rate” of 25% agrees with some other studies (19) and merits caution in interpreting data based solely on accessibility of chromatin and histone marks. However, some are bone-fide enhancers in other locations; for example Enh29, mapping about 70kb 5', is equivalent to “SOM”, an enhancer active in many tissues except the gonads (27). Others may have distinct roles; indeed Enh11 contains a putative CTCF binding site. In addition, several putative enhancers, notably Enh4, 5, 8, and 9, appear open in both granulosa and Sertoli cells, with Enh8 even more so in the former. These could contribute to the low level of *Sox9* seen in supporting cell precursors, but they may also represent sequences required to repress *Sox9*, which might not be detected by transgenic reporter assays.

The notion of redundancy or “shadow enhancers” within a regulatory region is well established (28, 29), and recent data suggests that deletion of single, even “ultraconserved” enhancers from developmentally important genes can have at most subtle if not undetectable effects (30, 31). It is therefore remarkable to see that deleting Enh13 alone phenocopies the loss of *Sox9* itself within the supporting cell lineage (9, 32). Substantial evidence points to the time-dependent action of SRY on *Sox9*. If *Sox9* fails to reach a critical threshold within a few hours then ovary-determining/anti-testis factors, such as Wnt signaling, accumulate to a sufficient level to repress *Sox9* and make it refractory to male promoting factors, including SRY, even though expression of the latter persists in XY gonads when Sertoli cells fail to differentiate (33). We suggest that Enh13 is an early acting enhancer, such that without it *Sox9* transcription fails to increase to a level where the other enhancers can act before the gene is silenced. It is only later that TES, and perhaps other enhancers such as Enh14, and Enh32, begin to act in a more redundant fashion, although it is conceivable that each has a major role to play during distinct phases of Sertoli cell development from the fetal to the

adult testis. It will be of interest to determine how Enh13 activity cascades into the recruitment of the other enhancers.

## Supplementary Material

Refer to Web version on PubMed Central for supplementary material.

## Acknowledgments

We are grateful to the Biological Research Facility, Genetic Modification Service, Advanced Sequencing Facility, and Experimental Histopathology Facility of the Francis Crick Institute and the Flow Cytometry Core at Northwestern University for technical assistance. We thank members of our labs for advice, support, and helpful comments.

**Funding:** This work was supported by the Francis Crick Institute which receives its core funding from Cancer Research UK (FC001107), the UK Medical Research Council (FC001107), and the Wellcome (FC001107); and by the UK Medical Research Council (U117512772). F.P. was funded by the Agence Nationale pour la Recherche (ANR blanc TestisDev). D.M.M. was funded by the Northwestern University School of Medicine.

## References

1. de Laat W, Duboule D. Topology of mammalian developmental enhancers and their regulatory landscapes. *Nature*. 2013; 502:499–506. [PubMed: 24153303]
2. Spitz F. Gene regulation at a distance: From remote enhancers to 3D regulatory ensembles. *Semin Cell Dev Biol*. 2016; 57:57–67. [PubMed: 27364700]
3. Garcia-Moreno SA, Plebanek MP, Capel B. Epigenetic regulation of male fate commitment from an initially bipotential system. *Mol Cell Endocrinol*. 2018
4. Capel B. Vertebrate sex determination: evolutionary plasticity of a fundamental switch. *Nat Rev Genet*. 2017; 18:675–689. [PubMed: 28804140]
5. Jakob S, Lovell-Badge R. Sex determination and the control of Sox9 expression in mammals. *FEBS J*. 2011; 278:1002–1009. [PubMed: 21281448]
6. Wilhelm D, Palmer S, Koopman P. Sex determination and gonadal development in mammals. *Physiol Rev*. 2007; 87:1–28. [PubMed: 17237341]
7. Koopman P, Gubbay J, Vivian N, Goodfellow P, Lovell-Badge R. Male development of chromosomally female mice transgenic for Sry. *Nature*. 1991; 351:117–121. [PubMed: 2030730]
8. Chaboissier MC, et al. Functional analysis of Sox8 and Sox9 during sex determination in the mouse. *Development*. 2004; 131:1891–1901. [PubMed: 15056615]
9. Barrionuevo F, et al. Homozygous inactivation of Sox9 causes complete XY sex reversal in mice. *Biol Reprod*. 2006; 74:195–201. [PubMed: 16207837]
10. Vidal VP, Chaboissier MC, de Rooij DG, Schedl A. Sox9 induces testis development in XX transgenic mice. *Nat Genet*. 2001; 28:216–217. [PubMed: 11431689]
11. Houston CS, et al. The campomelic syndrome: review, report of 17 cases, and follow-up on the currently 17-year-old boy first reported by Maroteaux et al in 1971. *Am J Med Genet*. 1983; 15:3–28. [PubMed: 6344634]
12. Foster JW, et al. Campomelic dysplasia and autosomal sex reversal caused by mutations in an SRY-related gene. *Nature*. 1994; 372:525–530. [PubMed: 7990924]
13. Wagner T, et al. Autosomal sex reversal and campomelic dysplasia are caused by mutations in and around the SRY-related gene SOX9. *Cell*. 1994; 79:1111–1120. [PubMed: 8001137]
14. Jo A, et al. The versatile functions of Sox9 in development, stem cells, and human diseases. *Genes Dis*. 2014; 1:149–161. [PubMed: 25685828]
15. Symon A, Harley V. SOX9: A genomic view of tissue specific expression and action. *Int J Biochem Cell Biol*. 2017; 87:18–22. [PubMed: 28323209]
16. Sekido R, Lovell-Badge R. Sex determination involves synergistic action of SRY and SF1 on a specific Sox9 enhancer. *Nature*. 2008; 453:930–934. [PubMed: 18454134]

17. Gonen N, Quinn A, O'Neill HC, Koopman P, Lovell-Badge R. Normal Levels of Sox9 Expression in the Developing Mouse Testis Depend on the TES/TESCO Enhancer, but This Does Not Act Alone. *PLoS Genet.* 2017; 13:e1006520. [PubMed: 28045957]
18. Maatouk DM, et al. Genome-wide identification of regulatory elements in Sertoli cells. *Development.* 2017; 144:720–730. [PubMed: 28087634]
19. Kvon EZ. Using transgenic reporter assays to functionally characterize enhancers in animals. *Genomics.* 2015; 106:185–192. [PubMed: 26072435]
20. Kim GJ, et al. Copy number variation of two separate regulatory regions upstream of SOX9 causes isolated 46,XY or 46,XX disorder of sex development. *J Med Genet.* 2015; 52:240–247. [PubMed: 25604083]
21. Correa SM, et al. Sex reversal in C57BL/6J XY mice caused by increased expression of ovarian genes and insufficient activation of the testis determining pathway. *PLoS Genet.* 2012; 8:e1002569. [PubMed: 22496664]
22. Sekido R, Bar I, Narvaez V, Penny G, Lovell-Badge R. SOX9 is up-regulated by the transient expression of SRY specifically in Sertoli cell precursors. *Dev Biol.* 2004; 274:271–279. [PubMed: 15385158]
23. Lee CH, Taketo T. Normal onset, but prolonged expression, of Sry gene in the B6.YDOM sex-reversed mouse gonad. *Dev Biol.* 1994; 165:442–452. [PubMed: 7958412]
24. Schmidt D, et al. The murine winged-helix transcription factor Foxl2 is required for granulosa cell differentiation and ovary maintenance. *Development.* 2004; 131:933–942. [PubMed: 14736745]
25. Rahmoun M, et al. In mammalian foetal testes, SOX9 regulates expression of its target genes by binding to genomic regions with conserved signatures. *Nucleic Acids Res.* 2017
26. Ohnesorg T, Croft B, Tan J, Sinclair AH. Using ROADMAP Data to Identify Enhancers Associated with Disorders of Sex Development. *Sex Dev.* 2016; 10:59–65. [PubMed: 27078861]
27. Mead TJ, et al. A far-upstream (-70 kb) enhancer mediates Sox9 auto-regulation in somatic tissues during development and adult regeneration. *Nucleic Acids Res.* 2013; 41:4459–4469. [PubMed: 23449223]
28. Lagha M, Bothma JP, Levine M. Mechanisms of transcriptional precision in animal development. *Trends Genet.* 2012; 28:409–416. [PubMed: 22513408]
29. Visel A, Rubin EM, Pennacchio LA. Genomic views of distant-acting enhancers. *Nature.* 2009; 461:199–205. [PubMed: 19741700]
30. Dickel DE, et al. Ultraconserved Enhancers Are Required for Normal Development. *Cell.* 2018; 172:491–499 e415. [PubMed: 29358049]
31. Osterwalder M, et al. Enhancer redundancy provides phenotypic robustness in mammalian development. *Nature.* 2018; 554:239–243. [PubMed: 29420474]
32. Lopes R, Korkmaz G, Agami R. Applying CRISPR-Cas9 tools to identify and characterize transcriptional enhancers. *Nat Rev Mol Cell Biol.* 2016; 17:597–604. [PubMed: 27381243]
33. Hiramatsu R, et al. A critical time window of Sry action in gonadal sex determination in mice. *Development.* 2009; 136:129–138. [PubMed: 19036799]
34. Beverdam A, Koopman P. Expression profiling of purified mouse gonadal somatic cells during the critical time window of sex determination reveals novel candidate genes for human sexual dysgenesis syndromes. *Hum Mol Genet.* 2006; 15:417–431. [PubMed: 16399799]
35. Buenrostro JD, Giresi PG, Zaba LC, Chang HY, Greenleaf WJ. Transposition of native chromatin for fast and sensitive epigenomic profiling of open chromatin, DNA-binding proteins and nucleosome position. *Nat Methods.* 2013; 10:1213–1218. [PubMed: 24097267]
36. McFarlane L, Truong V, Palmer JS, Wilhelm D. Novel PCR assay for determining the genetic sex of mice. *Sex Dev.* 2013; 7:207–211. [PubMed: 23571295]
37. van Galen P, et al. A Multiplexed System for Quantitative Comparisons of Chromatin Landscapes. *Mol Cell.* 2016; 61:170–180. [PubMed: 26687680]
38. Gasca S, et al. A nuclear export signal within the high mobility group domain regulates the nucleocytoplasmic translocation of SOX9 during sexual determination. *Proc Natl Acad Sci U S A.* 2002; 99:11199–11204. [PubMed: 12169669]

39. Turatsinze JV, Thomas-Chollier M, Defrance M, van Helden J. Using RSAT to scan genome sequences for transcription factor binding sites and cis-regulatory modules. *Nat Protoc.* 2008; 3:1578–1588. [PubMed: 18802439]
40. Ferraz-de-Souza B, et al. CHIP-on-chip analysis reveals angiopoietin 2 (Ang2, ANGPT2) as a novel target of steroidogenic factor-1 (SF-1, NR5A1) in the human adrenal gland. *FASEB J.* 2011; 25:1166–1175. [PubMed: 21163858]
41. Hartwig S, et al. Genomic characterization of Wilms' tumor suppressor 1 targets in nephron progenitor cells during kidney development. *Development.* 2010; 137:1189–1203. [PubMed: 20215353]
42. Mertin S, McDowall SG, Harley VR. The DNA-binding specificity of SOX9 and other SOX proteins. *Nucleic Acids Res.* 1999; 27:1359–1364. [PubMed: 9973626]
43. Murphy MW, Zarkower D, Bardwell VJ. Vertebrate DM domain proteins bind similar DNA sequences and can heterodimerize on DNA. *BMC Mol Biol.* 2007; 8:58. [PubMed: 17605809]
44. Yamagata T, et al. Of the GATA-binding proteins, only GATA-4 selectively regulates the human interleukin-5 gene promoter in interleukin-5-producing cells which express multiple GATA-binding proteins. *Mol Cell Biol.* 1995; 15:3830–3839. [PubMed: 7791790]

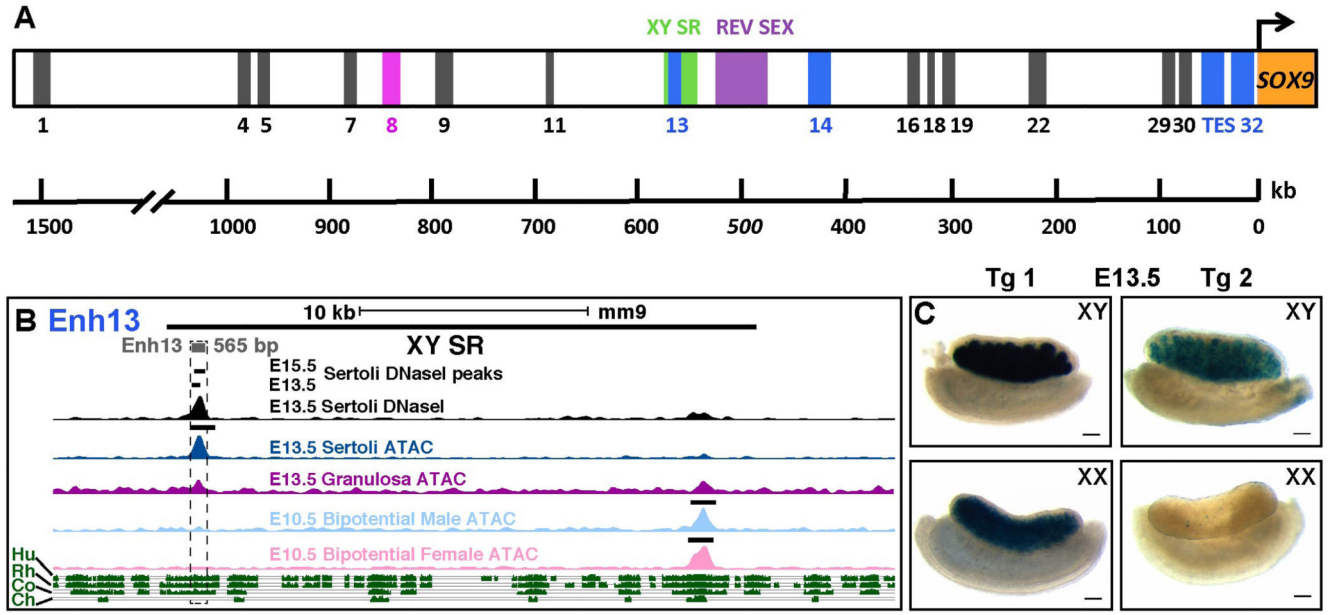


**Fig. 1. Enh13 is a testis-positive enhancer of *Sox9* located within the XY SR region.**

(A) A schematic representation of the gene desert upstream of the *mSox9* gene and the location of the putative enhancers identified by ATAC-seq and DNaseI-seq that were screened *in vivo* using transgenic reporter mice. Enhancers that did not drive gonad-expression of LacZ are shown in grey. Enhancers that drove testis-specific and ovary-specific LacZ expression are shown in blue and pink, respectively. The mouse regions that show conserved synteny with the human XY SR and REV SEX are depicted in green and purple boxes respectively. (B) Enh13 (grey box) is located at the 5' side of the 25.7 kb mouse equivalent XY SR locus (black rectangular box). DNaseI-seq (black) on E15.5 and E13.5 XY sorted Sertoli cells, and ATAC-seq on E13.5 sorted Sertoli cells (blue) and granulosa cells (purple) as well as E10.5 sorted somatic cells, at Enh13 genomic region are presented. Peaks correspond to nucleosome depleted regions, and are marked by black box if they are significantly enriched compared to flanking regions as determined by MACS, and present in at least two biological replicates. The grey box overlaying each peak indicates the cloned fragment. Green lines represent sequence conservation between mouse, human, rhesus, cow and chicken (sequence conservation tracks obtained from UCSC). (C)  $\beta$ -Gal staining (blue) of E13.5 testes and ovaries from two representative independent stable Enh13 transgenic lines. Scale bars represent 100  $\mu$ m.

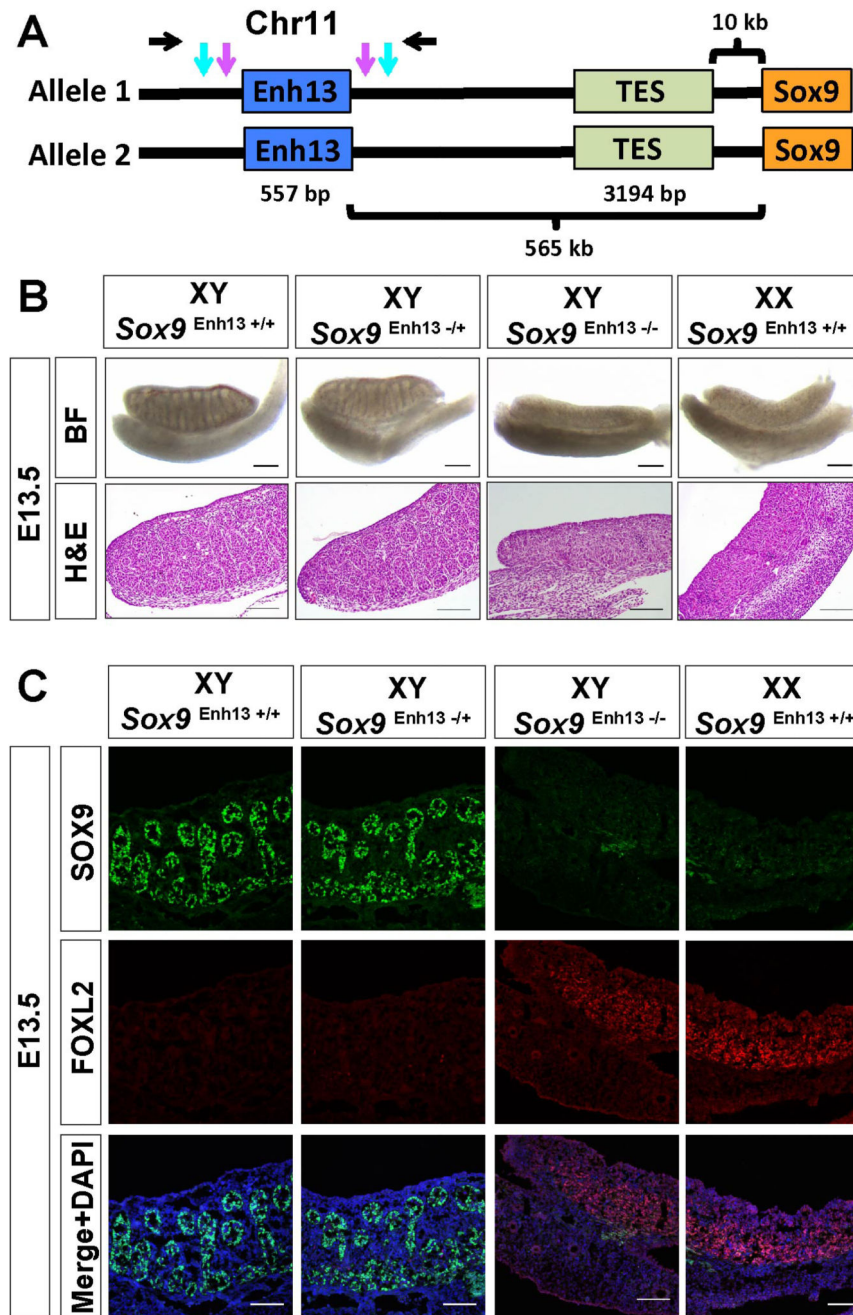


**Fig. 2. Deletion of *Enh13* leads to complete XY male-to-female sex reversal.**

(A) A schematic representation of the location of *Enh13* and TES upstream of *Sox9*. Turquoise and purple arrows represent the external and internal sgRNAs used to delete *Enh13*, respectively. Black arrows represent the PCR primers used to genotype *Enh13* deleted embryos and mice. (B) Bright field pictures and haematoxylin and eosin (H&E) stained sections of E13.5 XY *Enh13*<sup>+/+</sup>, *Enh13*<sup>+/-</sup> and *Enh13*<sup>-/-</sup> and XX *Enh13*<sup>+/+</sup> gonads. (C) Immunostaining of E13.5 gonads from XY wild type, *Enh13*<sup>+/-</sup>, *Enh13*<sup>-/-</sup> and XX wild type. Gonads were stained for Sertoli-marker SOX9 (green), granulosa-marker FOXL2 (red)

and DAPI (blue). Sex reversed gonads are indistinguishable from WT XX gonads, while the heterozygous deletion does not appear to alter testis morphogenesis. Scale bars represent 100  $\mu\text{m}$ .

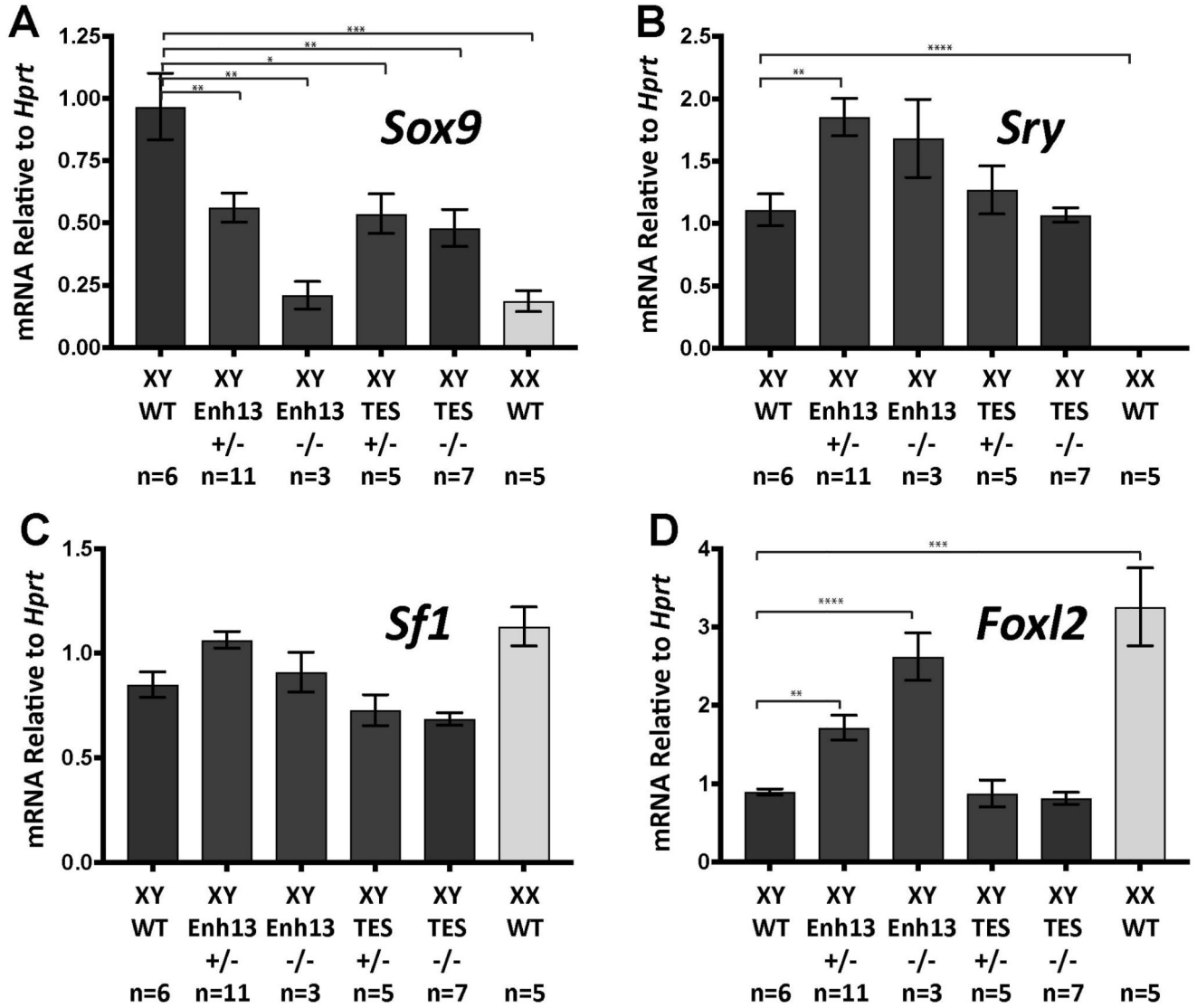


**Fig. 3. Enh13 regulates the expression of the *Sox9* gene *in vivo*.**

(A-D) Real-time quantitative PCR of genes involved in male (*Sox9*, *Sry*, *Sf1*) and female sex determination (*Foxl2* and *Sf1*) in XY Enh13 deleted and TES deleted gonads at E11.5 (18 tail somites). Data are presented as mean  $2^{-Ct}$  values, normalized to the housekeeping gene *Hprt*. Sample size represents the number of individuals and is indicated below each genotype. Error bars show SEM of  $2^{-Ct}$  values. P value is presented above the relevant bars (unpaired, two-tailed t-test on  $2^{-Ct}$  values, \*P 0.05, \*\*P 0.01, \*\*\*P 0.001, \*\*\*\*P 0.0001). Dark grey bars: XY; light grey bars: XX.

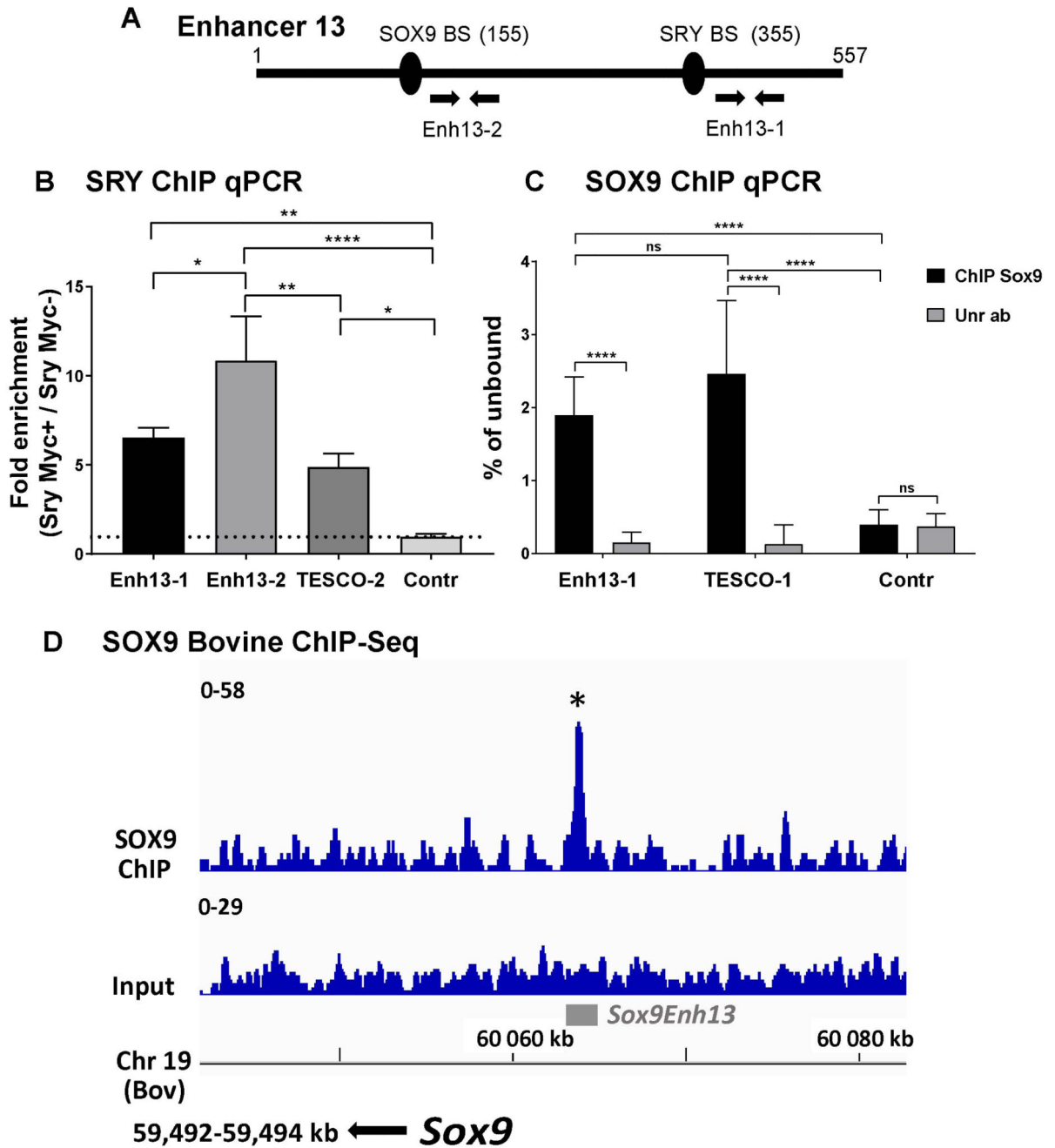


**Fig. 4. Enh13 is bound by SRY and SOX9 *in vivo*.**

(A) A schematic representation of the location of the primers used for ChIP experiments in Enh13 (B) ChIP-qPCR assay of E11.5 mouse genital ridge following immunoprecipitation with anti-cMYC antibody. Data is presented as fold enrichment of SRY-MYC positive relative to SRY-MYC negative genital ridges, meaning that values greater than 1 represent specific enrichment. The primers used span the putative SRY binding site in Enh13, TESCO (Around SRY R6 site, see (16)) and a negative control region on Chr11. Data are the mean  $\pm$  SD (n = 2); \*\*\*\* P < 0.0005 (Student t test). (C) ChIP-qPCR assay of E13.5 mouse testes

following immunoprecipitation with anti-SOX9 antibody. The primers used span the putative SOX9 binding site in Enh13, TESCO (Around SOX9 R1 site, see (16)) and a negative control region on Chr11. Data are the mean  $\pm$  SD (n = 3); \*\*\*\* P<0.0005 (Student t test). (D) ChIP-seq with anti-SOX9 antibody using E90 foetal bovine testis. The bovine Enh13 is indicated by the grey box (at Cow Bostau8 chr19: 60,063,628-60,064-165). The star represents the peaks with FDR <0.05 in the two bovine datasets. Y Axis numbers represent counts. The input tracks represent sequencing reads of chromatin input. The *bSox9* gene is indicated by the arrow and is 570 kb downstream (to the left) of Enh13.